



# Modeling and simulation of dye-sensitized solar cell: Model verification for different semiconductors and dyes



Aghareed M. Tayeb<sup>a</sup>, Ahmed A.A. Solyman<sup>b</sup>, Mohamed Hassan<sup>c,\*</sup>,  
Tamer M. Abu el-Ella<sup>d</sup>

<sup>a</sup> Faculty of Engineering, Minia University, Minia, Egypt

<sup>b</sup> Department of Electrical and Electronics Engineering, Faculty of Engineering and Architecture, Istanbul Gelisim University, Turkey

<sup>c</sup> Chemical Engineering Department, College of Engineering, Jazan University, Jazan, Saudi Arabia

<sup>d</sup> Technical Research Center, Cairo, Egypt

Received 13 October 2021; revised 6 February 2022; accepted 25 February 2022

## KEYWORDS

P–V and I–V curve;  
Photovoltaic cell;  
Simulation;  
Dye-sensitized solar cell (DSSC);  
Matlab/Simulink

**Abstract** In this article, the use of MATLAB/SIMULINK interface to realize a generalized photovoltaic simulation model is introduced. The model was created utilizing the photovoltaic (PV) cell fundamental circuit equations, including the effects of solar radiation and variations in temperature. This modeling approach enables the I–V and P–V curve of PV cells to be understood. It could also be used as a tool to forecast the behavior of any solar PV cell under differing environmental circumstances (e.g., temperature, irradiation conditions). These effects are simultaneously added in real-time. Due to their nonlinear features, they must be modeled to design and simulate the maximum power point of solar cells. This model applies to dye-sensitized solar cells with three different semiconductors, namely, TiO<sub>2</sub>, ZnO, and SnO<sub>2</sub>; use N3 dye. According to changes in atmospheric parameter values such as solar radiation, temperature, and operating parameter values like semiconductor type, dye concentration, and particles, the characteristic dimensions of photovoltaic systems such as power supply voltage (PV) and current–voltage (I–V) characteristics are drawn; in the MATLAB/SIMULINK interface observed. The simulation results reveal that these elements and the respective photovoltaic model affect the maximum operating performance of PV modules. The battery made of TiO<sub>2</sub> semiconductor and N3 dye showed the greatest consistency with the model battery, followed by the battery made of ZnO, and finally, the battery made of SnO<sub>2</sub> with the same dye N3.

© 2022 THE AUTHORS. Published by Elsevier BV on behalf of Faculty of Engineering, Alexandria University. This is an open access article under the CC BY-NC-ND license (<http://creativecommons.org/licenses/by-nc-nd/4.0/>).

\* Corresponding author.

E-mail addresses: [aghareed1@yahoo.com](mailto:aghareed1@yahoo.com) (A.M. Tayeb), [mihassan@jazanu.edu.sa](mailto:mihassan@jazanu.edu.sa) (M. Hassan).

Peer review under responsibility of Faculty of Engineering, Alexandria University.

<https://doi.org/10.1016/j.aej.2022.02.057>

1110-0168 © 2022 THE AUTHORS. Published by Elsevier BV on behalf of Faculty of Engineering, Alexandria University. This is an open access article under the CC BY-NC-ND license (<http://creativecommons.org/licenses/by-nc-nd/4.0/>).

## 1. Introduction

Photovoltaic cells are considered the basic energy conversion unit of photovoltaic power generation systems. The operating curves of solar systems under various operating situations are costly and time-consuming. Photovoltaic cells have nonlinear properties. Single models of solar power systems have been developed and included in numerous engineering applications to solve this challenge. Adjusted models have been modified and different according to the kind of software that scientists use, such as C Programming, Excel, Matlab/Simulink, or their toolboxes. Matlab supports both numeric and symbolic modeling approaches and provides curve fitting, statistics, optimization, ODE and PDE solving, calculus, and other core mathematical tools. Simulink adds an environment for modeling and simulating the behavior of multidomain systems and for developing embedded systems. A function for computing current, voltage, solar radiation, and temperature data was developed in the Matlab environment [1,2]. The reliability of several PV models was checked by bearing in mind the correction errors of certain data points [3].

One of these models is a reverse bias model, which is used to clarify the temperature effect on PV cell performance [4]. The other model is a detailed terminal stress model suggested using a five-parameter model [5–7]. Four-parameter and five-parameter models [8] and [9] evaluated single-crystal photovoltaic modules. The suggested model is built by employing common modules inside the Simulink environment in [10–13] based on solar cells and arrays' mathematical equations. The influence of environmental (solar and temperature) conditions and physical factors (diode factor, series resistance;  $R_s$ , shunt resistance; saturation current and  $R_{sh}$ ), etc. were explored in these investigations.

The work in the Simscape/Simulink environment of the work of [14,15] utilized solar cell blocks. With this module, the manufacturer provides input parameters such as short-circuit current, open-circuit voltage, etc. This approach has the disadvantage of not assessing certain parameters, for example, saturation current and temperature. In [16,17] and other investigations, the solar model constructed with labeling tools in the Simulink environment has been documented. This study addressed only two issues (solar radiation and temperature) and did not provide a step-by-step modeling process. On the other hand, considering thermal convection, thermal radiation, and power generation, some temperature-dependent models for photovoltaic module operation have been proposed [18–20]. Commercial PV modules have demonstrated temperature dependence experiments in panel energy and efficiency [9,21–23]. The battery current is the specific value of the specific battery operating temperature and corresponding solar radiation [24,2]. The voltage and current output of the photovoltaic generator will fluctuate if the temperature and solar radiation change accordingly. Thus, variations in temperature and intensity of the solar radiation should be incorporated in the last photovoltaic model. The inclusion of these effects in modeling PV generators was mentioned in [25–27]. The method is to obtain a model of known temperature and known solar radiation intensity and to address various temperature values and levels of radiation. The battery's operating temperature will also change, resulting in a new output voltage and the new photocurrent value of the ambient temperature and radiation

intensity change. These influences of the battery output voltage and battery current are represented by the  $K_i$  and  $K_o$  coefficients in the model [21,28]. Some studies studied nanocomposites synthesized based on metal frame work [29–32].

Many studies were conducted regarding simulation PV modules by [33–35]. However, the main difference in the above research is that the effects of partial shadowing on solar modules are not taken into account.

This model evaluate parameters that can greatly affect the I-V and P-V characteristics of PV cells, including physical parameters such as saturation current, ideality factor, series and parallel strength, and environmental circumstances the proposed model will aid (solar radiation, temperature, and shadow effects).

## 2. Experimental work

The author has conducted experimental studies on many DSSCs made of various nanoscale semiconductors and various dyes. The results show that, compared with N917 and black dye, N3 dye provides the highest cell performance, so modeling studies will be performed on cells made with N3 dye. Regarding semiconductor types,  $TiO_2$  nanomaterials (particle size 5 nm) provide the highest battery performance, followed by ZnO, and finally  $SnO_2$ . Therefore, the Matlab/Simulink simulation model was verified for the three semiconductor/dye combinations that achieve the highest performance; B.  $TiO_2$ /N3, ZnO/N3, and  $SnO_2$ /N3. Battery performance is evaluated based on maximum output current ( $I_{max}$ ), maximum output power ( $P_{max}$ ), and efficiency.

The characteristic equations of PV/solar cell voltage and current (VI) are calculated by a series of equations as follows:

### Determination of $I_{ph}$ :

$$I_{ph} = [I_{sc} + K_i(T_{op} - T_{ref})][G/1000] \quad (1)$$

$I_{ph}$ , Photocurrent, A;  $I_{sc}$ , Short circuit current (current when the voltage is zero), A;  $K_i$  "Short circuit temperature coefficient";  $T_{op}$  "Operating temperature", K;  $T_{ref}$  "Reference temperature", K;  $G$  The PV modeling illumination,  $W/m^2$ .

### Determination of $I_{rs}$ :

$$I_{rs} = (I_{sc}) / (\exp[(q * V_{oc}) / (NsKAT_{op})] - 1) \quad (2)$$

$I_{rs}$  "reverse saturation current", A;  $q$  "Electron charge ( $1.6 * 10^{-19}$  °C)";  $V_{oc}$  "Open circuit voltage" (the voltage when current is zero), V;  $Ns$  "Number of cells connected in Series";  $K$  "Boltzman's constant ( $1.3805 * 10^{-23}$ )" and  $A$  "Ideality factor".

### Determination of $I_s$ :

$$I_s = [I_{rs}(T_{op}/T_{ref})^3][\exp(qE_g((1/T_{ref}) - (1/T_{op}))) / (KA)] \quad (3)$$

$I_s$  Current in  $R_{sh}$  resistance, A;  $I_{rs}$  Module reverse saturation current, A;  $E_g$  The bandgap, eV and  $K$  "Boltzman's constant ( $1.3805 * 10^{-23}$ )".

### Determination of $I_o$ :

$$I_o = N_p I_{ph} - N_p I_{ph} [\exp((qV_o + I_o R_s) / (N_s A K T)) - 1] - [(V_o) + (I_o * R_s)] / (R_{sh}) \quad (4)$$

$I_o$  Total output current, A;  $N_p$  "Number of cells connected in parallel";  $V_o$  "Output voltage", V;  $R_s$  "Series resistance of PV module",  $\Omega$  and  $R_{sh}$  "parallel resistance of PV module".

This paper is research on the simulation and modeling of dye-sensitized photovoltaic cells via the MATLAB/Simulink interface model. The simulation model is validated for three types of semiconductor nanomaterials, such as B. TiO<sub>2</sub>, ZnO, and SnO<sub>2</sub> and N3 dyes. The IV and PV features of the model cell's PV cell and the controlled cell are shown.

The three batteries tested were named C1, C2, and C3, as shown in Table 1.

2.1. Mathematical modeling of the solar cell

Mathematical equivalent circuit:

To create the model and assess the model parameters while performing, we use the basic circuit equations of photovoltaic (PV) solar cells indicated in equation (4) (in the introduction to this study). Current I is determined by using the normal electrical properties of the battery (I<sub>sc</sub>, V<sub>oc</sub>) and variables: voltage irradiance (G) (T). The model reflects the effects and temperature fluctuations of solar radiation.

2.2. Experimental setup

Matlab/Simulink Interface:

The experimental photovoltaic test system setup is an equivalent photovoltaic cell circuit used to verify the Matlab/Simulink model. The equivalent photovoltaic cell circuit (Fig. 1). A PV cell can be represented in parallel by a current source I<sub>ph</sub>, which is coupled to a diode, as while it has lit, it creates current and acts as a diode when not illuminated. The circuit model equivalent also contains a shunt and a range of internal strengths (Fig. 1). R<sub>s</sub> and R<sub>sh</sub> are resistors. The R<sub>sh</sub> value is generally considerably larger than that of R<sub>s</sub>. While R<sub>s</sub> is relatively small that can be omitted to facilitate the analysis. Fig. 2 shows the experimental apparatus. The system consists of a rheostat, a solar radiometer, two digital multimeters, and a battery-composed solar system. The specifications are listed in Table 2.

Reference cell:

1000 W solar cells are utilized as a referral cell simulation, the detailed cell specifications are provided in Table 2.

The simulation model's input parameters are:

T<sub>ref</sub>: Reference temperature value = 298.15 K.

K: Boltzman's constant = 1.3805\*10<sup>-23</sup> J/K.

K<sub>t</sub>: Short circuit temperature coefficient = 0.0013.

A: Ideality factor = 1.2.

E<sub>g</sub>: Band gap energy = 1.1 eV.

R<sub>s</sub>: Is the series resistor, normally the value of this one is very small = 0.0001 Ω.

R<sub>sh</sub>: Parallel resistance of PV module = 1000 Ω.

q: Electron charge = 1.6\*10<sup>-19</sup> C.

I<sub>sc</sub>: PV module with 25 °C and 1000 W/m<sup>2</sup> short circuit current = 5.711 mA.

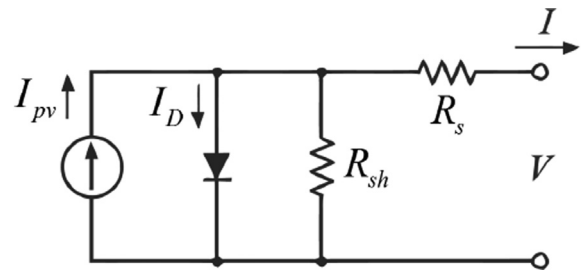


Fig. 1 The equivalent PV cell circuit model.



Fig. 2 The experimental setup of the solar simulation system.

Table 2 DS-100 M PV module data\* on electrical characteristics.

DS-100 M	Name
Maximum voltage (V <sub>max</sub> )	0.436 V
Maximum current (I <sub>max</sub> )	5.1 mA
Maximum power (P <sub>max</sub> )	2.223 W
Range of operating temperature	-15 °C to 60 °C

\* The electrical requirements are subject to 1 kW/m<sup>2</sup> irradiation test circumstances, 1.5 air mass spectrum, and 25 °C cell temperature.

V<sub>oc</sub>: PV module open circuit voltage at 298.15 K and 1000 W/m<sup>2</sup> = 0.577 V.

3. Results and discussion

Because of the nonlinear characteristics of photovoltaic modules, it is necessary to model them to design and simulate max-

Table 1 Characteristics of DSSCs tested with Matlab/Simulink model.

Nomination of Cell	Type of Semiconductor	Type of Dye	I <sub>max</sub> , A	P <sub>max</sub> , W	The efficiency of the resulting cell, %
C1	TiO <sub>2</sub>	N3	5.1	2.223	5.56
C2	ZnO	N3	3.61	1.660	4.15
C3	SnO <sub>2</sub>	N3	3.42	1.504	3.76

imum power point tracking (MPPT) for photovoltaic system applications.

3.1. Model calculation of the solar system equations

The modeled equivalent circuit is shown in Fig. 3.

The simulation calculation models of  $I_{ph}$ ,  $I_{rs}$ ,  $I_s$ , and  $I_o$  (according to Eqs. (1)–(4)) are shown in Figs. 4–7.

3.2. Matlab simulation of P-V and I-V characteristics of the PV cell

(Model validation):

The model of the PV cell is realized by the Matlab program. During execution, equations from 1 to 4 were used to evaluate the model parameters for the experimental test system. The program also uses the typical electrical parameters ( $I_{sc}$ ,  $V_{oc}$ ) and variables of the battery or module: irradiance (G), voltage, and temperature (T) to determine the current I.

The test results and empirical results are recorded under the conditions of an irradiation intensity of  $1000 \text{ W/m}^2$  and an operating temperature of  $40 \text{ }^\circ\text{C}$ .

3.2.1. Characteristic curve Current-voltage (IV) curve and characteristic curve

The power-voltage (PV) characteristic curve is displayed according to the solar radiation and temperature values specified in the MATLAB/Simulink interface. For the three photovoltaic cell

types tested, the results of this simulation method are shown in Figs. 8–10; C1, C2, and C3 (as described in Table 1). These figures show the empirical results of the MATLAB/Simulink interface simulation model (simulation (IV) curve and simulation (PV) curve) and the characteristic curve (IV) and (PV) curve of the generated PV cell) (see Tables 3–5).

Table 6 shows the experimental data and empirical simulation data of PV cells C1, C2, and C3. The P-V and I-V simulations and experimental findings for short circuit current, open-circuit tensions, and maximum power output can be seen from Figs. 8–10 and Table 6.

Therefore, the MATLAB/Simulink simulation model is suitable for DSSC. The consistency of cell C1 made of  $\text{TiO}_2/\text{N3}$  is closer, followed by cell C2 made of  $\text{ZnO}/\text{N3}$ , and finally cell C3 made of  $\text{SnO}_2/\text{N3}$ .

3.3. Simulation results under changing solar irradiation and temperature

Another simulation study was conducted to study the effects of temperature changes (with constant solar radiation) and changes in solar radiation (with constant temperature) on the characteristics of the battery C1.

3.3.1. Effect of changing the temperature at constant solar irradiation

Using the software simulation model Matlab/Simulink to simulate the IV and PV characteristics of the PV cell is carried out

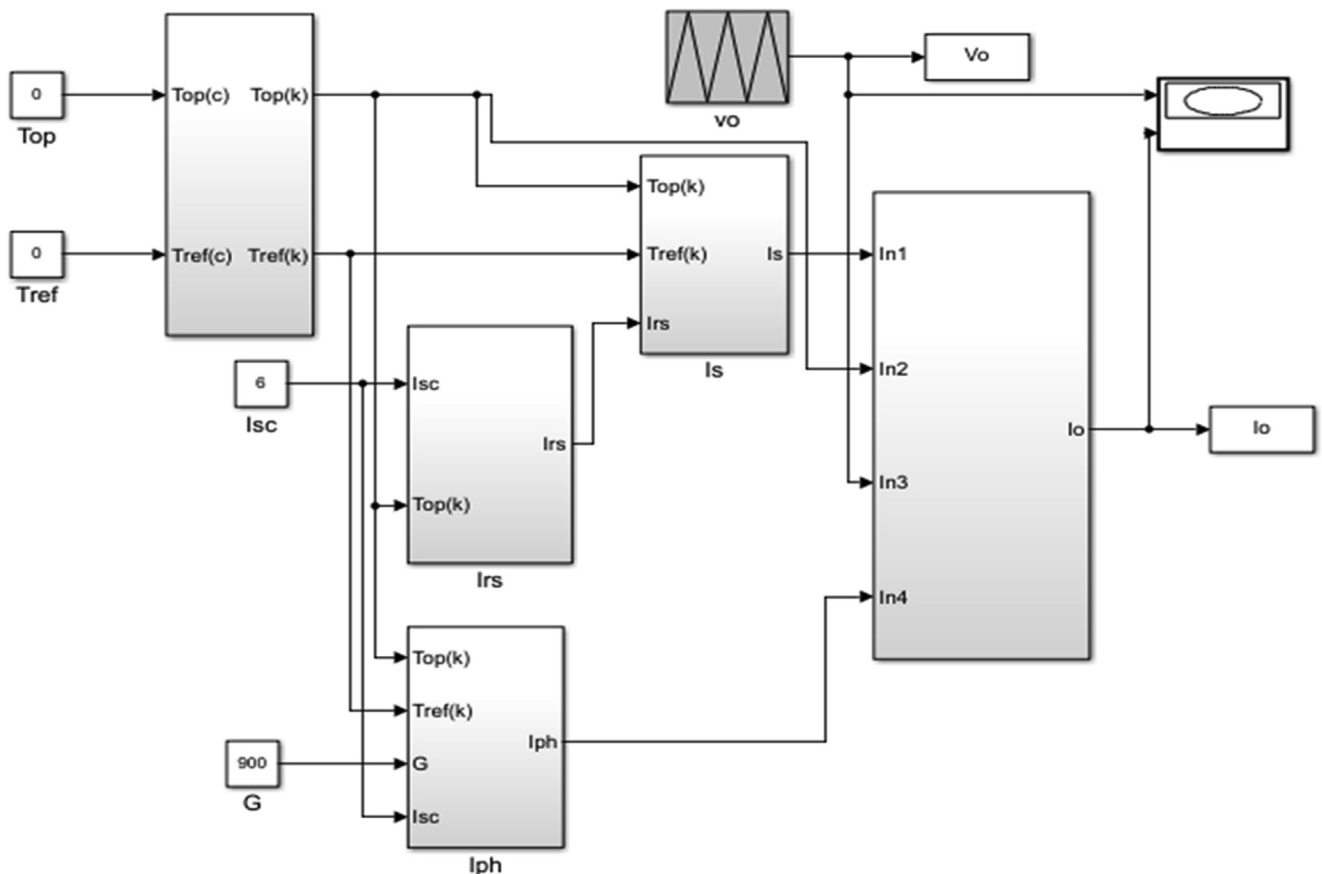


Fig. 3 The modeled equivalent circuit of Fig. 1.

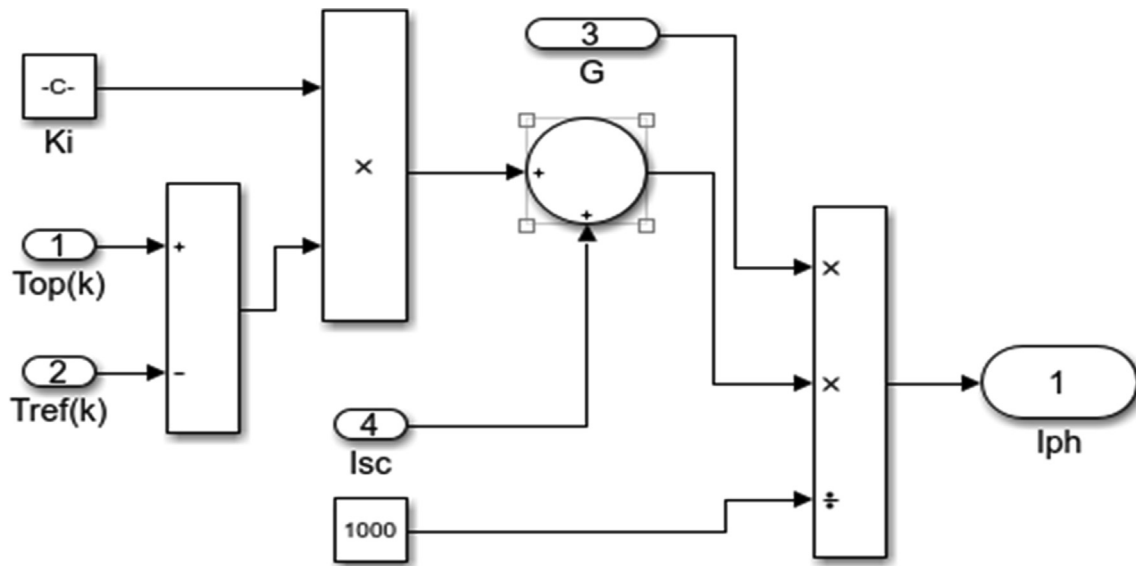


Fig. 4 The modeled circuit of Eq. (1),  $I_{ph}$  (Photocurrent).

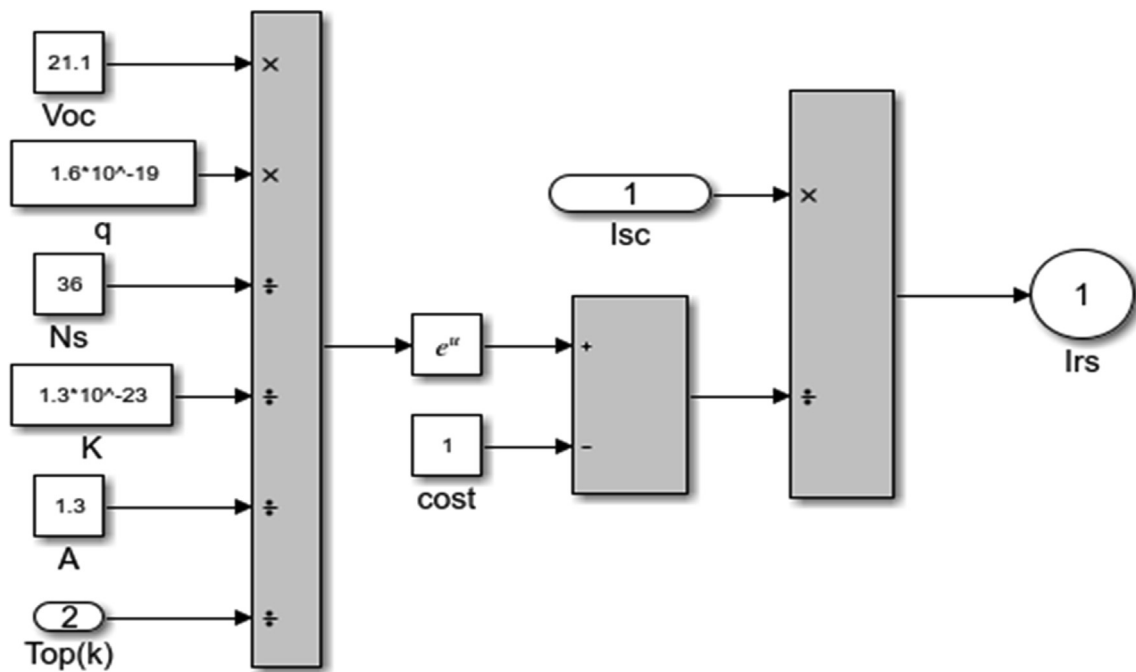


Fig. 5 The modeled circuit of Eq. (2),  $I_{rs}$ (Reverse saturation current).

at different operating temperatures, while the solar radiation intensity remains constant at  $1000 \text{ W/m}^2$ . The operating temperatures tested are 25, 50, and  $75 \text{ }^\circ\text{C}$ . The IV and PV characteristics are shown in Fig. 1 and Fig. 2. Examination of these figures showed that:

- If the operational temperature falls, the output power and voltage rise, while the current remains virtually unchanged.

- The current output increased marginally when the working temperature increased, but the output voltage decreased sharply. As the temperature increased, the net power output decreased.

Therefore, changes in ambient temperature have a significant impact on open-circuit voltage and maximum output power. The open-circuit voltage values are 0.3, 0.43, and  $0.54 \text{ V}$ , and the ambient temperature is 75, 50, and  $25 \text{ }^\circ\text{C}$ .

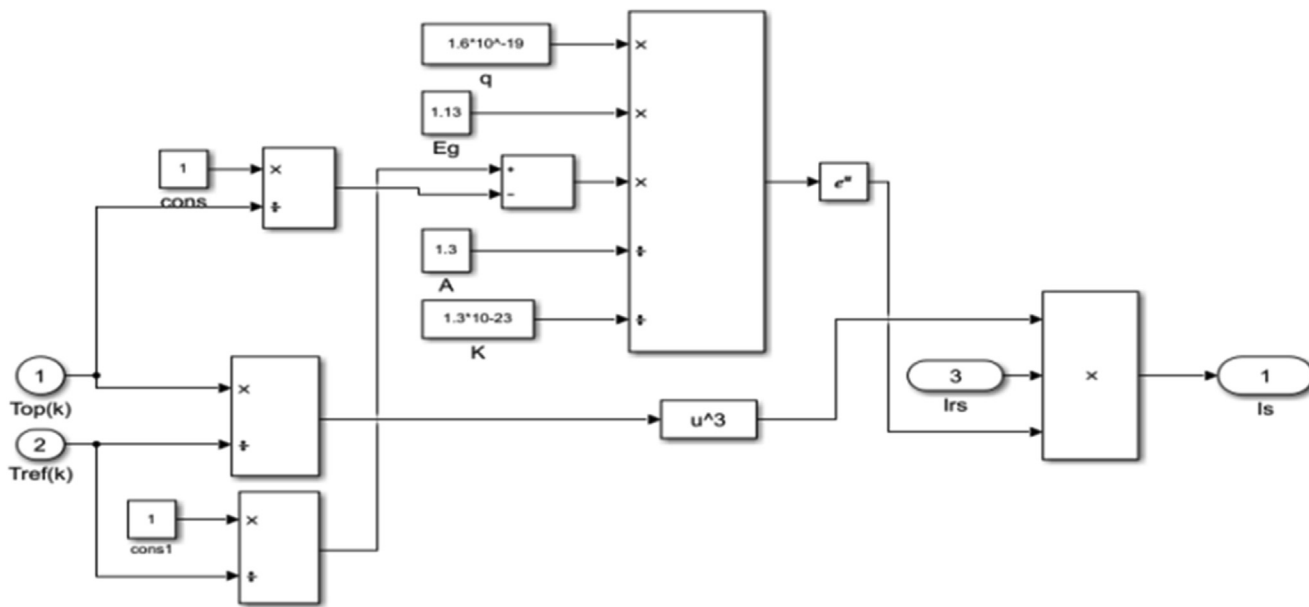


Fig. 6 The modeled circuit of Eq.3,  $I_s$  (Current in  $R_{sh}$  resistance).

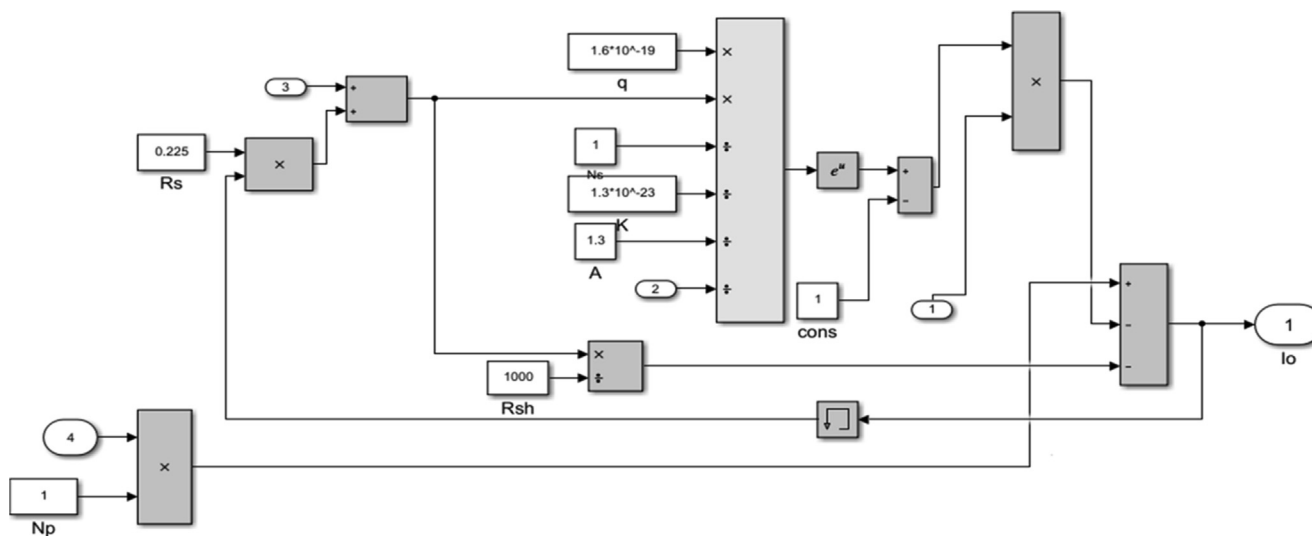


Fig. 7 The modeled circuit of Eq. (4),  $I_o$  (Total output current).

With the increase in ambient temperature, the short circuit current increased significantly, but this increase is not enough to compensate for the loss of power caused by an open circuit voltage drop. Maximum voltage;  $V_{max} = 0.409$  V and maximum output power;  $P_{max} = 2.041$  mW realized at an ambient temperature of 25 °C (see Figs. 11 and 12).

3.3.2. Effect of changing solar irradiation at a constant temperature

Simulate photovoltaic cells under various solar radiation levels; B. 400, 700, and 1000  $W/m^2$  and a constant ambient temperature of 25 °C.

The results of these tests are graphically displayed as the IV and PV characteristics in Figs. 13 and 14, respectively. Exam-

ination of these figures showed that the model’s output features correspond to the DS100M solar cell characteristics. The output power, current, and voltage are reduced when the solar radiation is reduced from 1000 to 400  $W/m^2$ . This means that at a fixed temperature, as the irradiation increased, the short-circuit current  $I_{sc}$  increased, which will lead to an increase in power output under these operating conditions. This seems logical and is the expected behavior of the solar energy conversion system. The maximum current value is  $V_{max} = 5.36$  mA, which is obtained when the solar radiation intensity is 1000  $W/m^2$ .

At a fixed ambient temperature of 25 °C and solar irradiation intensity of 1000  $W/m^2$  the values recorded are: short circuit current ( $I_{sc}$ ) = 5.36 mA, maximum current



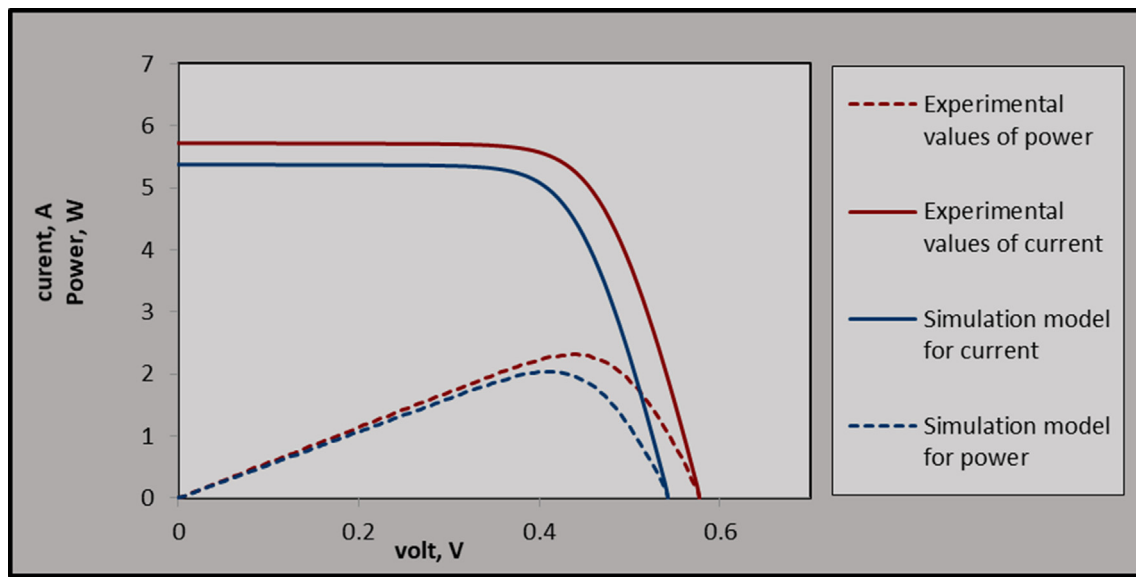


**Fig. 8** Simulation model and experimental (P-V), (I-V) characteristics curves (MATLAB/Simulink simulation model and characteristics figure of cell C1).

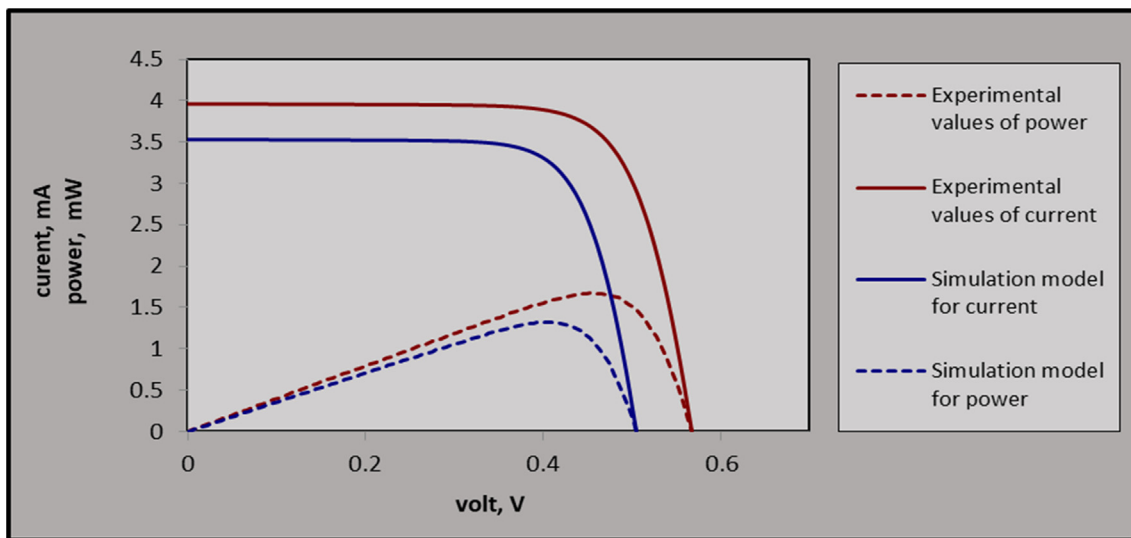


**Fig. 9** Simulation model and experimental (P-V), (I-V) characteristic curves (MATLAB/Simulink simulation model and characteristics figure of cell C2).

$(I_{max}) = 4.98 \text{ mA}$ , and maximum voltage ( $V_{max}) = 0.409 \text{ V}$ . These corresponds to the maximum power ( $P_{max}) = 2.041 \text{ mW}$ .

The short-circuit current is proportional to solar radiation, showing the predicted response to radiation changes by the characteristic curve of Fig. 13. Fig. 14 displays the variation

in solar ( $G$ ) radiation characteristic curve (PV) while the ambient temperature ( $T_a$ ) is maintained constantly at  $25 \text{ }^\circ\text{C}$ . The increase in the intensity of solar radiation increased the maximal capacity.

The suggested model also has extra advantages and may therefore be used to examine the effects of environmental fac-

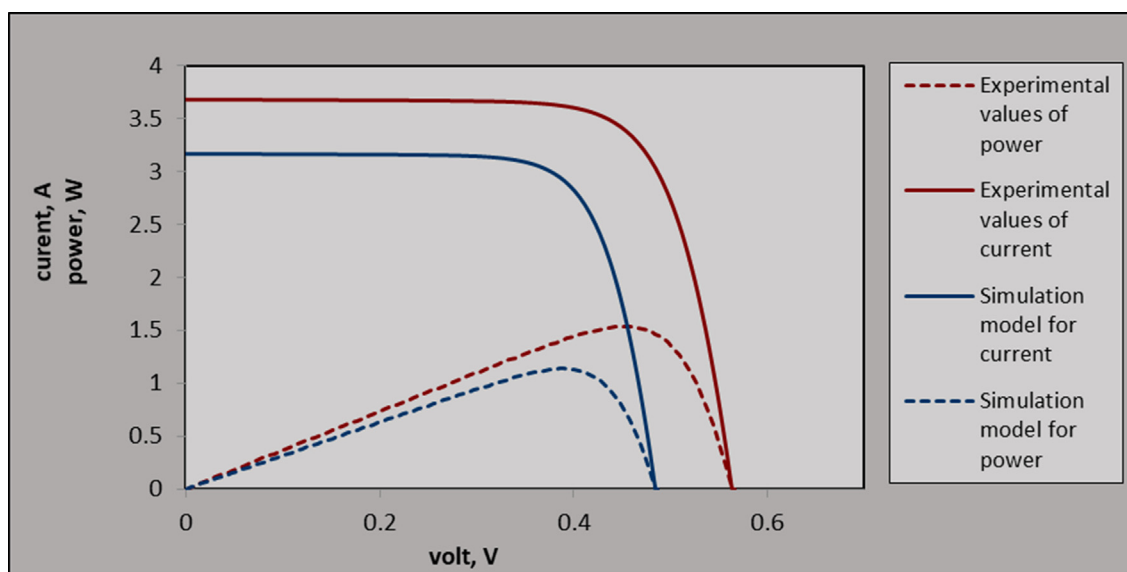


**Fig. 10** Simulation model and experimental (I-V), (P-V) Characteristics curves (Matlab/Simulink simulation model and characteristics figure of cell C3).

**Table 3** Simulation model and experimental (P-V), (I-V) characteristics data of cell C1 ( $\text{TiO}_2/\text{N}_3$ ).

Parameter	$I_{sc}$ , A	$V_{oc}$ , V	$V_{max}$ , V	$I_{max}$ , A	$P_{max}$ , W	F. F	Eff., %
Practical cell data	5.711	0.577	0.436	5.1	2.223	67.10	5.56
Model data	5.372	0.543	0.413	4.8	2.13	64.68	5.34

**Table 4** Simulation model and experimental (P-V), (I-V) characteristic data of cell C2 ( $\text{ZnO}/\text{N}_3$ ).

Parameter	$I_{sc}$ , A	$V_{oc}$ , V	$V_{max}$ , V	$I_{max}$ , A	$P_{max}$ , W	F. F	Eff., %
Practical cell data	3.96	0.56	0.46	3.61	1.66	73.87	4.15
Model data	3.52	0.5	0.41	3.21	1.47	65.75	3.69

( $\text{SnO}_2/\text{N}_3$ ).

**Table 5** Simulation model and experimental (P-V), (I-V) characteristics data of cell C2.

Parameter	$I_{sc}$ , A	$V_{oc}$ , V	$V_{max}$ , V	$I_{max}$ , A	$P_{ma}$ , W	F. F	Eff., %
Practical cell data	3.6	0.56	0.44	3.42	1.5	72.66	3.76
Model data	3.1	0.48	0.35	2.77	1.21	58.85	3.04



**Table 6** Experimental and simulated data for cells C1, C2, and C3.

Parameter	Cell Type					
	C1		C2		C3	
	Experimental data	Simulated data	Experimental data	Simulated data	Experimental data	Simulated data
$I_{sc}$ , A	5.71	5.37	3.96	3.52	3.6	3.1
$V_{oc}$ , V	0.57	0.54	0.56	0.5	0.56	0.48
$V_{max}$ , V	0.436	0.41	0.46	0.41	0.44	0.35
$I_{max}$ , A	5.1	4.89	3.61	3.21	3.42	2.77
$P_{max}$ , W	2.22	2.13	1.66	1.47	1.5	1.21
F.F	67.38	64.68	73.87	65.75	72.66	58.85
	5.55	5.33	4.15	3.69	3.76	3.04
Efficiency, %	96%		89%		81%	

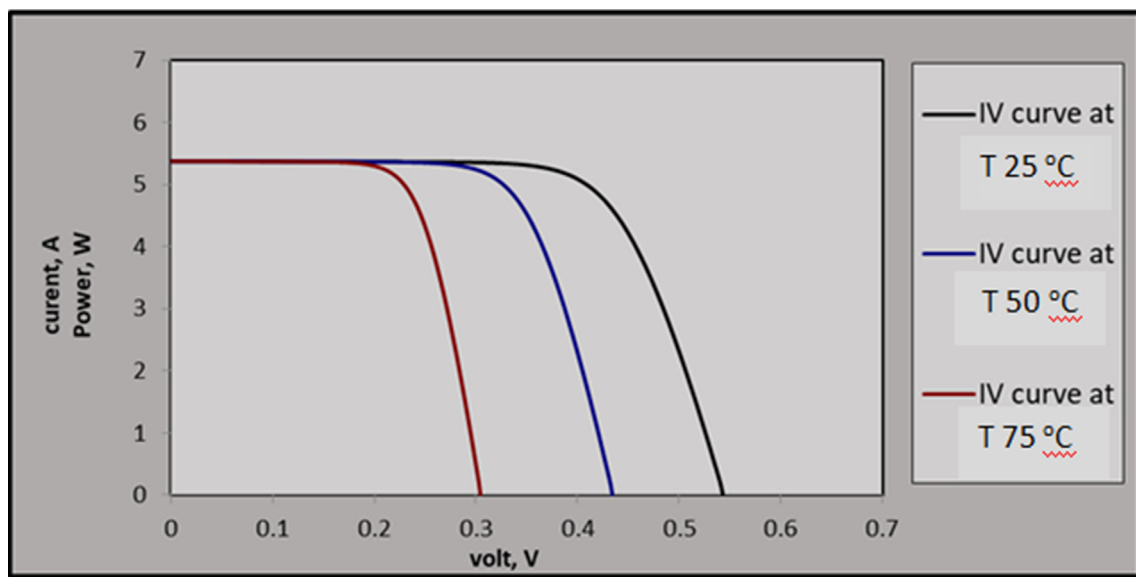


**Fig. 11** Output I-V curve with varying temperature.

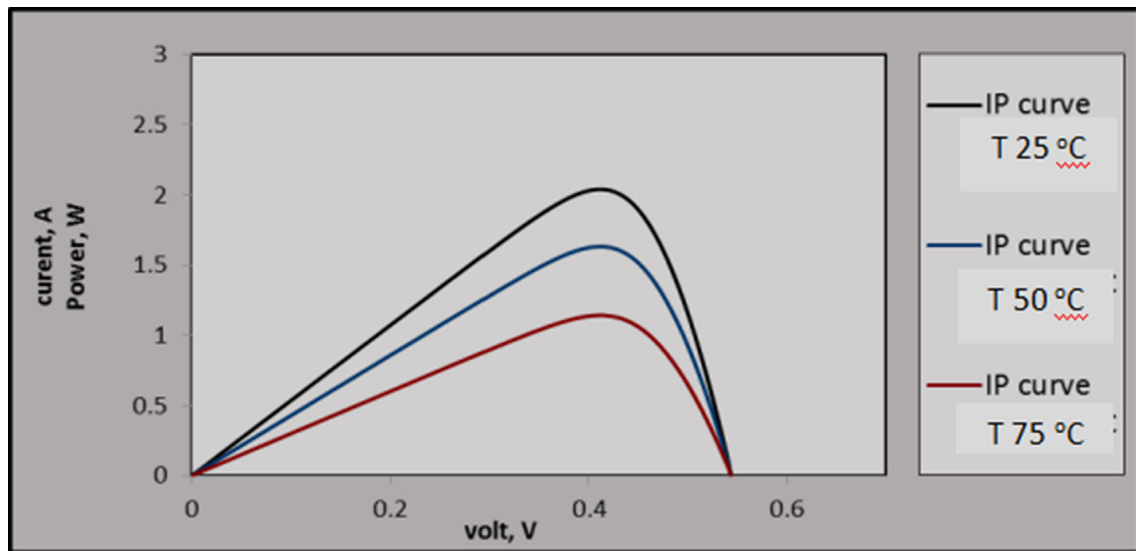


**Fig. 12** Output P-V curve with varying temperature.

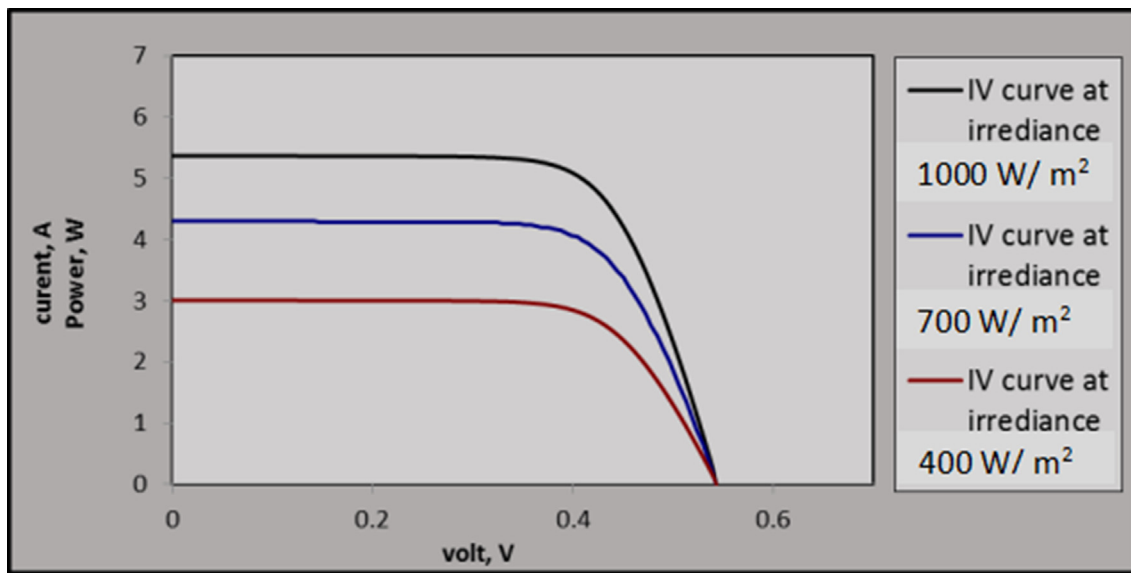


Fig. 13 Output I-V curve with the varying irradiation intensity.

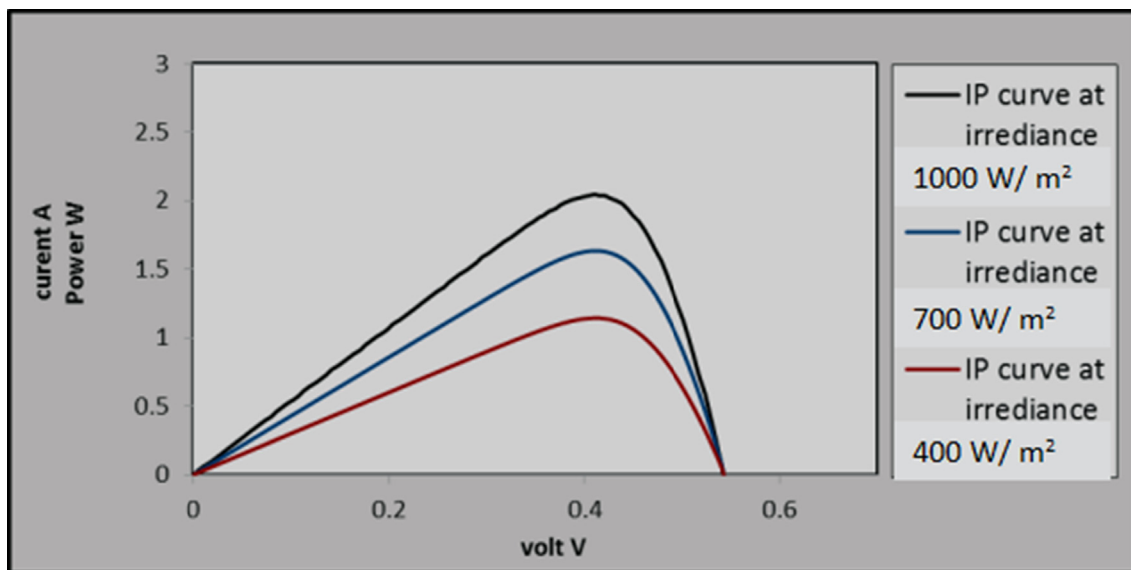


Fig. 14 Output P-V curve with the varying irradiation intensity.

tors, for example, temperature and solar radiation changes, and the effect of physical characteristics, such as series resistance,  $R_s$ , and shunt resistance  $R_{sh}$ .

#### 4. Conclusion

The obtained results from modeling and experiments were drawn from the current study. Using the MATLAB/Simulink model, a PV model is created based on the mathematical equations of solar cells. This model is used to simulate a PV cell with MATLAB/Simulink block libraries with a step-by-step process. This modeling approach enables the I-V and P-V curve of PV cells to be understood. It could also be used as a tool to forecast the behavior of any solar PV cell under differing environmental circumstances (e.g., temperature, irradiation conditions). The change in the environmental

parameter is considered as input data in this situation, whereas the output data are considered for the I-V and P-V characteristics. Results indicated that the output curves of the model match the DS-100 M solar cell characteristics. This has a considerable effect on the open-circuit voltage and maximum output power changes in ambient temperature. The findings have shown that when solar irradiation falls from 1000 to 100  $W/m^2$ , output power, current, and voltage decrease. The output power and voltage are increased by lowering the ambient temperature, however, the output current maintains virtually constant.

#### 5. Availability of data and materials

Any data concerning this article are available from the corresponding author on request.

## Funding

No external funding sources other than the facilities of Minia University, Minia, Egypt, are required.

## Declaration of Competing Interest

The authors declare that they have no known competing financial interests or personal relationships that could have appeared to influence the work reported in this paper.

## Acknowledgment

The authors would like to acknowledge the sincere support of Dr. AmrKmalHrfosh, former head of Renewable Energy Lab., Technical Research Center, Cairo, Egypt. His valuable help in dealing with the simulator and other instruments and his collaborative efforts in the supervision of the study has been a great support for finishing this work.

## References

- [1] G. Walker, Evaluating MPPT converter topologies using a matlab PV model, *J. Electr. Electron. Eng. Aust.* 21 (2001) 49–55.
- [2] F. Gonzalez-Longatt, Model of Photovoltaic Module in Matlab, II CIBELEC. (2006). file:///C:/Users/44737/Downloads/Model\_of\_Photovoltaic\_Module\_in\_Matlab.pdf.
- [3] M. de Blas, J. Torres, E. Prieto, A. García, Selecting a suitable model for characterizing photovoltaic devices, *Renew. Energy.* 25 (2002) 371–380, [https://doi.org/10.1016/S0960-1481\(01\)00056-8](https://doi.org/10.1016/S0960-1481(01)00056-8).
- [4] M.C. Alonso-García, J.M. Ruiz, Analysis and modelling the reverse characteristic of photovoltaic cells, *Sol. Energy Mater. Sol. Cells.* 90 (7-8) (2006) 1105–1120, <https://doi.org/10.1016/j.solmat.2005.06.006>.
- [5] W. De Soto, S.A. Klein, W.A. Beckman, Improvement and validation of a model for photovoltaic array performance, *Sol. Energy.* 80 (1) (2006) 78–88, <https://doi.org/10.1016/j.solener.2005.06.010>.
- [6] R. Chenni, M. Makhlof, T. Kerbache, A. Bouzid, A detailed modeling method for photovoltaic cells, *Energy.* 32 (9) (2007) 1724–1730, <https://doi.org/10.1016/j.energy.2006.12.006>.
- [7] M.T. Sarniak, Modeling the functioning of the half-cells photovoltaic module under partial shading in the matlab package, *Appl. Sci.* 10 (2020) 1–12, <https://doi.org/10.3390/app10072575>.
- [8] A.N. Celik, N. Acikgoz, Modelling and experimental verification of the operating current of mono-crystalline photovoltaic modules using four- and five-parameter models, *Appl. Energy.* 84 (1) (2007) 1–15, <https://doi.org/10.1016/j.apenergy.2006.04.007>.
- [9] J.-H. Jung, S. Ahmed, Real-time simulation model development of single crystalline photovoltaic panels using fast computation methods, *Sol. Energy.* 86 (6) (2012) 1826–1837, <https://doi.org/10.1016/j.solener.2012.03.003>.
- [10] T. Salmi, M. Bouzguenda, A. Gastli, M. a., MATLAB Simulink Based Modeling of Solar Photovoltaic Cell, *Int. J. Renew. Energy Res.* 2 (2012) 213–218.
- [11] S. Panwar, R. Saini, Development and Simulation of Solar Photovoltaic model using Matlab/simulink and its parameter extraction, in: *Int. Conf. Comput. Control Eng.*, 2012, pp. 1–8.
- [12] S. Nema, R. Nema, G. Agnihotri, Matlab/simulink based study of photovoltaic cells/modules/array and their experimental verification, *Int. J. Energy Environ.* 1 (2010) 487–500. [http://www.ijee.ieefoundation.org/vol1/issue3/IJEE\\_09\\_v1n3.pdf](http://www.ijee.ieefoundation.org/vol1/issue3/IJEE_09_v1n3.pdf).
- [13] P. Sudeepika, G.G. Khan, Analysis Of Mathematical Model Of PV Cell Module in Matlab/Simulink Environment, *Int. J. Adv. Res. Electr. Electron. Instrum. Energy.* 3 (2014) 7823–7829. <https://www.semanticscholar.org/paper/Analysis-Of-Mathematical-Model-Of-PV-CellModule-in-P.Sudeepika-Khan/d3a5ad439c239410361d2f8eaa240cf92edde69>.
- [14] M.S. Ibbini, S. Mansi, M. Masadeh, E.I.D.A.L. Hajri, Simscape solar cells model analysis and design, *Comput. Appl. Environ. Sci. Renew. Energy.* (2014) 97–103.
- [15] M.G. Venkateswarlu, P. Sangameswarlu, Simscape model of photovoltaic cell, *Int. J. Adv. Res. Electr. Electron. Instrum. Eng.* 2 (2013) 2278–8875, [www.ijareeie.com](http://www.ijareeie.com).
- [16] A. Varshney, A. Tariq, Simulink model of solar array for photovoltaic power generation system, *Int. J. Electr. Electr. Eng.* 7 (2014) 8.
- [17] S. Mohammed, Modeling and simulation of photovoltaic module using Matlab/Simulink, *Int. J. Chem. Environ. Eng.* 2 (2011). <https://memberfiles.freewebs.com/34/73/75277334/documents/Individual.pdf>.
- [18] Y. Sukamongkol, S. Chungpaibulpatana, W. Ongsakul, A simulation model for predicting the performance of a solar photovoltaic system with alternating current loads, *Renew. Energy.* 27 (2) (2002) 237–258, [https://doi.org/10.1016/S0960-1481\(02\)00002-2](https://doi.org/10.1016/S0960-1481(02)00002-2).
- [19] A.D. Jones, C.P. Underwood, A thermal model for photovoltaic systems, *Sol. Energy.* 70 (4) (2001) 349–359, [https://doi.org/10.1016/S0038-092X\(00\)00149-3](https://doi.org/10.1016/S0038-092X(00)00149-3).
- [20] P. Bevilacqua, S. Perrella, R. Bruno, N. Arcuri, An accurate thermal model for the PV electric generation prediction: long-term validation in different climatic conditions, *Renew. Energy.* 163 (2021) 1092–1112, <https://doi.org/10.1016/j.renene.2020.07.115>.
- [21] G.M. Tina, R. Abate, Experimental verification of thermal behaviour of photovoltaic modules, in: MELECON 2008 - 14th IEEE Mediterr. Electrotech. Conf., IEEE, 2008, pp. 579–584, <https://doi.org/10.1109/MELCON.2008.4618497>.
- [22] O. Gil-Arias, E.I. Ortiz-Rivera, A general purpose tool for simulating the behavior of PV solar cells, modules and arrays, in: 11th IEEE Work. Control Model. Power Electron. COMPEL 2008, 2008, <https://doi.org/10.1109/COMPEL.2008.4634686>.
- [23] E. Skoplaki, J.A. Palyvos, On the temperature dependence of photovoltaic module electrical performance: A review of efficiency/power correlations, *Sol. Energy.* 83 (5) (2009) 614–624, <https://doi.org/10.1016/j.solener.2008.10.008>.
- [24] V. Perraki, P. Kounavis, Effect of temperature and radiation on the parameters of photovoltaic modules, *J. Renew. Sustain. Energy.* 8 (1) (2016) 013102, <https://doi.org/10.1063/1.4939561>.
- [25] R.A. Gupta, R. Kumar, A.K. Bansal, BBO-based small autonomous hybrid power system optimization incorporating wind speed and solar radiation forecasting, *Renew. Sustain. Energy Rev.* 41 (2015) 1366–1375, <https://doi.org/10.1016/j.rser.2014.09.017>.
- [26] H. Rezk, N. Kanagaraj, M. Al-Dhaifallah, Design and sensitivity analysis of hybrid photovoltaic-fuel-cell-battery system to supply a small community at Saudi NEOM city, *Sustain.* 12 (8) (2020) 3341.
- [27] A. Chauhan, S. Upadhyay, M.T. Khan, S.M.S. Hussain, T.S. Ustun, Performance investigation of a solar photovoltaic/diesel generator based hybrid system with cycle charging strategy using BBO algorithm, *Sustain.* 13 (14) (2021) 8048, <https://doi.org/10.3390/su13148048>.
- [28] D. Guerra, E. Iakovleva, N. Vatin, P. Zunino, E. Vdovin, Mathematical modeling of parameters of solar modules for a solar power plant 2.5 MW in the climatic conditions of the

- Republic of Cuba, E3S Web Conf. 140 (2019) 04013, <https://doi.org/10.1051/e3sconf/201914004013>.
- [29] P. Nasehi, M.S. Moghaddam, S.F. Abbaspour, N. Karachi, Preparation and characterization of a novel Mn-Fe<sub>2</sub>O<sub>4</sub> nanoparticle loaded on activated carbon adsorbent for kinetic, thermodynamic and isotherm surveys of aluminum ion adsorption, *Sep. Sci. Technol.* 55 (6) (2020) 1078–1088, <https://doi.org/10.1080/01496395.2019.1585456>.
- [30] M. Saei Moghaddam, J. Towfighi, Vanadium oxide supported on Al-modified Titania nanotubes for oxidative dehydrogenation of propane, *J. Chem. Pet. Eng.* 51 (2017) 113–121.
- [31] M.S. Moghaddam, J. Towfighi, Synthesis of vanadium catalysts supported on cerium containing TiO<sub>2</sub> nanotubes for the oxidative dehydrogenation of propane, *Pet. Chem.* 58 (8) (2018) 659–665, <https://doi.org/10.1134/S0965544118080170>.
- [32] P. Nasehi, B. Mahmoudi, S.F. Abbaspour, M.S. Moghaddam, Cadmium adsorption using novel MnFe<sub>2</sub>O<sub>4</sub>-TiO<sub>2</sub>-UIO-66 magnetic nanoparticles and condition optimization using a response surface methodology, *RSC Adv.* 9 (35) (2019) 20087–20099.
- [33] D. Jena, V.V. Ramana, Modeling of photovoltaic system for uniform and non-uniform irradiance: A critical review, *Renew. Sustain. Energy Rev.* 52 (2015) 400–417, <https://doi.org/10.1016/j.rser.2015.07.079>.
- [34] M. Madhukumar, T. Suresh, M. Jamil, Investigation of photovoltaic grid system under non-uniform irradiance conditions, *Electron.* 9 (2020) 1–23, <https://doi.org/10.3390/electronics9091512>.
- [35] X.H. Nguyen, M.P. Nguyen, Mathematical modeling of photovoltaic cell/module/arrays with tags in Matlab/Simulink, *Environ. Syst. Res.* 4 (1) (2015), <https://doi.org/10.1186/s40068-015-0047-9>.